Biosensors and Bioelectronics 77 (2016) 372–377

Contents lists available at ScienceDirect

Biosensors and Bioelectronics

journal homepage: www.elsevier.com/locate/bios

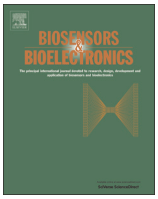

Nickel/cobalt oxide-decorated 3D graphene nanocomposite electrode for enhanced electrochemical detection of urea

Nhi Sa Nguyen, Gautam Das, Hyon Hee Yoon*

Department of Chemical and Bio Engineering, Gachon University, Gyeonggi-do 461-701, Republic of Korea

ARTICLE INFO

Article history:
Received 19 June 2015
Received in revised form
6 September 2015
Accepted 21 September 2015
Available online 25 September 2015

Keywords:
Urea sensor
Non-enzymatic
Ni–Co oxide
3D graphene
Urine

ABSTRACT

A $NiCo_2O_4$ bimetallic electro-catalyst was synthesized on three-dimensional graphene (3D graphene) for the non-enzymatic detection of urea. The structural and morphological properties of the $NiCo_2O_4$/3D graphene nanocomposite were characterized by X-ray diffraction, Raman spectroscopy, and scanning electron microscopy. The $NiCo_2O_4$/3D graphene was deposited on an indium tin oxide (ITO) glass to fabricate a highly sensitive urea sensor. The electrochemical properties of the prepared electrode were studied by cyclic voltammetry. A high sensitivity of $166\ \mu A\ mM^{-1}\ cm^{-2}$ was obtained for the $NiCo_2O_4$/3D graphene/ITO sensor. The sensor exhibited a linear range of 0.06–0.30 mM ($R^2 = 0.998$) and a fast response time of approximately 1.0 s with a detection limit of 5.0 μM. Additionally, the sensor exhibited high stability with a sensitivity decrease of only 5.5% after four months of storage in ambient conditions. The urea sensor demonstrates feasibility for urea analysis in urine samples.

1. Introduction

Urea, a metabolic end product in the human body, is critical in assessing various metabolic disorders, including renal function (Singh et al., 2008). Moreover, monitoring of urea levels is important in the food and environmental industries. Chromatographic and spectroscopic methods (Boggs et al., 2009) have been widely employed to measure urea concentrations in biological and chemical samples. However, these methods require tedious sample preparation and cannot be used on-site. Alternative methods using various biosensors based on the urease enzyme have been developed, with simple designs capable of rapid on-site urea analysis. The enzymatic hydrolysis of urea generates NH_4^+ and HCO_3^- ions (Eq. (1)), which can be amperometrically (Tiwari et al., 2009; Velichkova et al., 2011; Yang et al., 2004), potentiometrically (Saeedfar et al., 2013), optically (Borisov and Wolfbeis, 2008), thermally (Malecha et al., 2009), and piezoelectrically (Yang et al., 2007) detected using various transducers (Cheng et al., 2013).

$$CO(NH_2)_2 + H_2O \rightarrow 2NH_3 + CO_2 \tag{1}$$

Amperometric biosensing is considered the most promising approach, because it offers a fast, reliable, simple, and low-cost detection (Das and Yoon, 2015; Luo and Do, 2004). In urease-based amperometric biosensors, the NH_4^+ ion can be catalytically oxidized by either a second enzyme (Srivastava et al., 2011) or metal catalysts (Singh et al., 2008; Hao et al., 2015). However, denaturing of the enzyme can cause poor long-term stability.

Recently, non-enzymatic biosensors with metal-based catalysts have received widespread interest for the high sensitivity and stability of the devices. Metal oxides such as NiO, CuO, and ZnO, with low costs and well-defined redox properties, have been employed for direct electro-catalytic oxidation and determination of many biochemical compounds such as urea (Vedharathinam and Botte, 2012), glucose (Ding et al., 2010), and ethanol (Holzinger et al., 2012). In particular, Ni-based catalysts have exhibited excellent catalytic abilities for urea oxidation (Choi et al., 2012; Tyagi et al., 2013; Wang et al., 2013). The electrochemical oxidation of urea at Ni-based electrodes in alkaline media can occur through the following reactions (Miao et al.,2014):

$$NiO + OH^- \leftrightarrows NiOOH + e^- \tag{2}$$

$$Ni(OH)_2 + OH^- \leftrightarrows NiOOH + e^- \tag{3}$$

$$CO(NH_2)_2 + 6OH^- \underset{NiOOH}{\rightarrow} N_2 + 5H_2O + CO_2 + 6e^- \tag{4}$$

Ni-based catalysts are limited by the participation of Ni in the oxygen evolution reaction (OER) at alkaline pH. This drastically reduces the efficiency of the catalytic oxidation of urea (Eq. (5)) (Vidotti et al., 2008):

$$4OH^- \rightarrow 4e^- + 2H_2O + O_2 \tag{5}$$

The OER has been reported to occur with the formation of β-phase $Ni(OH)_2$ in alkaline media (Vidotti et al., 2008). However, using a mixed Co–Ni hydroxide, the OER was significantly

---

* Corresponding author. Fax: +82 31 750 5363.
E-mail address: hhyoon@gachon.ac.kr (H.H. Yoon).

http://dx.doi.org/10.1016/j.bios.2015.09.046
0956-5663/© 2015 Elsevier B.V. All rights reserved.

suppressed (Vidotti et al., 2008). The inclusion of Co in the Ni structure may also enhance the conductivity and shift the oxidation peaks to less positive values.

A major concern barring the usage of Ni–Co oxide electrodes is the structural degradation and expansion during the course of electrochemical reactions, which severely limits the applicability of the material as a catalyst. Several authors reported the use of carbon nanotubes (CNT) as structural supports to enhance the sensitivity and stability of such oxide-based catalysts (Holzinger et al., 2012; Luo et al., 2001). Graphene, which has a higher surface area and similar thermal and electrical conductivities compared to CNT (Jiang and Fan, 2014), has also been used as a catalyst support (O'Hayre et al., 2006). Recently, Co oxide deposited on three-dimensional (3D) graphene was reported to show excellent performance in non-enzymatic glucose detection (Dong et al., 2012). The 3D graphene formed a continuous conductive interconnected network, eliminating the formation of inter-sheet junctions, and thus eased the diffusion of analytes through porous structures (Zhang et al., 2014).

In the present investigation, a novel electrode employing Ni–Co oxides deposited on 3D graphene was prepared for the non-enzymatic sensing of urea. The structural, morphological, and electrochemical properties of the Ni–Co oxides-3D graphene nanocomposite electrode were investigated.

2. Experimental

2.1. Materials

Ni foam was purchased from E2 TECH Co., Korea (NiP200, 340 mm × 150 mm × 1.5 mm, 110 ppi). Nickel nitrate hexahydrate (98.5%) and cobalt nitrate hexahydrate (98%) were purchased from Sigma-Aldrich, Korea. All other chemicals used in the present investigation were of reagent grade.

2.2. Preparation of $Ni_xCo_{3-x}O_4$/3D graphene nanocomposites

The $Ni_xCo_{3-x}O_4$/3D graphene nanocomposite was prepared by the following two steps. Firstly, 3D graphene was prepared by chemical vapor deposition (CVD), similar to previous reports (Chen et al., 2011; Lin et al., 2005; Zhang et al., 2014). Ni foam with dimensions of 2 cm × 2 cm was used as the catalyst and as a scaffold for the graphene network growth. A 3D graphene foam was obtained by etching the Ni scaffold with 3 M HCl. $Ni_xCo_{3-x}O_4$ with different Ni/Co ratios was deposited on the 3D graphene foam by hydroxide thermal decomposition (Yan et al., 2012). The 3D graphene was homogeneously dispersed in ethylene glycol by ultrasonication. To this dispersion, pre-calculated amounts of nickel (II) nitrate and cobalt (II) nitrate solution in ethylene glycol were added and stirred for 1 h at room temperature, after which NaOH in ethylene glycol was added while stirring vigorously. The precipitated 3D graphene and Ni–Co hydroxide slurry was filtered and washed with de-ionized (DI) water. It was then heated at 350 °C for 3 h to decompose the metal hydroxides into the metal oxide $Ni_xCo_{3-x}O_4$ on the 3D graphene foam. For comparison testing, a $NiCo_2O_4$/CNT composite was also prepared by the same protocol.

2.3. Preparation of the electrodes

The electrodes were fabricated by a vacuum-assisted sequential deposition technique. A 1 mg/mL $Ni_xCo_{3-x}O_4$/3D graphene dispersion in dimethylformamide (DMF) was passed through an Anodisc membrane fitted to a suction filter apparatus. The $Ni_xCo_{3-x}O_4$/3D graphene-deposited Anodisc membrane was air-dried and placed on a 5 mm × 20 mm indium tin oxide (ITO) glass substrate. The $Ni_xCo_{3-x}O_4$/3D graphene–ITO electrodes were obtained by etching the Anodisc membrane with 0.5 NaOH solution, followed by repeated washing with DI water and vacuum drying in an oven at 35–40 °C for 24 h. A polyion complex (PIC) of 5 μL aqueous poly-L-lysine (PLL, 75 mmol/L monomer unit) and 5 μL aqueous polystyrene sulfonate (PSS, 60 mmol/L monomer unit) was drop-cast sequentially on $Ni_xCo_{3-x}O_4$/3D graphene/ITO to form an encapsulating membrane. The electrode was dried at room temperature overnight and stored in a vacuum desiccator prior to electrochemical analysis.

2.4. Analysis

The 3D graphene and $NiCo_2O_4$/3D graphene were analyzed by Raman spectroscopy using a micro-Raman spectrometer (Dongwoo Optron Olympus Mono-Ra500i, S. Korea) equipped with a 10 × objective lens and a laser excitation wavelength of 633 nm. Powder X-ray diffraction (XRD) analysis of the samples was performed using an X-ray diffractometer (Rigaku D/MAX-2200, Japan) with Cu-Kα radiation at a wavelength of 1.5406 Å. The morphological characteristics and compositional analysis of the 3D graphene and $NiCo_2O_4$/3D graphene were performed by a scanning electron microscope (SEM, Hitachi S-4700; Hitachi Ltd., Tokyo, Japan) equipped with an energy dispersive X-ray spectroscope (EDX).

The electrochemical measurements of the electrodes were performed at ambient conditions in a three-compartment cell using a potentiostat-galvanostat (VSP, BioLogic-Science Instruments, 38640 CLAIX, France) in a Tris–HCl buffer solution (pH 8.0). A conventional three-electrode system using Pt wire, Ag/AgCl, and $Ni_xCo_{3-x}O_4$/3D graphene as the counter, reference, and working electrodes, respectively, was used for the measurements.

3. Results and discussion

3.1. Characterization of $NiCo_2O_4$/3D graphene

The structure of the as-prepared $NiCo_2O_4$/3D graphene nanocomposite was analyzed by Raman spectroscopy. Fig. 1(a) shows the Raman spectrum of the $NiCo_2O_4$/3D graphene nanocomposite. The Raman spectrum displays the characteristic G band at ~1580 cm^{-1} corresponding to the sp^2-bonded planar C atoms and a 2D band at approximately 2712 cm^{-1} indicating crystalline graphite (Dresselhaus et al., 2010). However, no obvious D band is seen in the spectrum, indicating that the graphene structure is free of defects. Several other peaks are also observed at 418, 448, 540, 716, and 728 cm^{-1}, corresponding to Co–O and Ni–O vibrations (Lin et al., 2005; Zhong et al., 2012).

Fig. 1(b) depicts the XRD patterns of 3D graphene and the $NiCo_2O_4$/3D graphene nanocomposites. The 3D graphene exhibits two prominent peaks at $2\theta=26.5°$ and 54.5°, attributed to the (002) and (004) Bragg reflections, respectively, of graphitic carbon (Lin et al., 2005). The reflection peaks of graphene and $NiCo_2O_4$ are observed in the diffractogram from the $NiCo_2O_4$/3D graphene nanocomposite. The peaks are indexed to the (111), (220), (222), (400), (331), (422), and (511) planes of spinel-structured $NiCo_2O_4$ (JCPDS-73-1702).

The morphology of the 3D graphene and $NiCo_2O_4$/3D graphene nanocomposites was observed by SEM. The porous 3D structure of graphene with single-layer-thick sheets interconnected into a skeleton is distinctly visible in Fig. 2(a). The 3D graphene structure correlates to a macroporous structure with pore sizes of ~50 nm. The bimetallic oxides seen in the micrographs as small white spots are uniformly dispersed on the 3D graphene network (Fig. 2(b)). The particles exhibit a uniform size with an average diameter of